Roller Chain-Like Robot For Steel Bridge Inspection

Son Thanh Nguyen[1], Hung Manh La[2]

[1,2] Advanced Robotics and Automation Lab, Department of Computer Science and Engineering, University of Nevada, Reno – NV89557, USA, Corresponding Email: hla@unr.edu

Abstract

This paper presents a novel design of steel bridge/structure inspection robot. Compared to most existing robots designed to work on particular surface contour of steel structures such as flat or curving, the proposed roller chain-like robot can implement and transfer smoothly on many kind of steel surfaces. The developed robot can be applied to inspection tasks for steel bridges with complicated structures. The robot is able to carry cameras, sensors for visual and specialized examination. Rigorous analysis of robot kinematics, adhesion force and turn-over failure has been conducted to demonstrate the stability of the proposed design. Mechanical and magnetic force analysis together with turn-over failure investigation can serve as an useful framework for designing various steel climbing robots in the future. Experimental results and field deployments prove the adhesion, climbing, inspection capability of the developed robot.

1. Introduction

Steel structures and bridges are important components of the civil infrastructures, which need to be regularly inspected to early detect defects for timely, efficient and less costly cure. There are more than 50,000 steel bridges in the United States (FHWA, 2016), which are in poor condition (either deficient or functionally obsolete). The current practice of inspection is mainly manual and needs a team of rope-certified bridge engineers to climb on high steel structures to perform visual inspection, which is dangerous and less efficient. For example, the most recent inspection of the Golden Gate bridge can be seen in (Golden Gate Bridge, 2018). There has been continuing efforts to provide automated inspection solutions using robots. For instance, magnetic wheel-based climbing robots have been developed (La et al., 2019), (Pham & La, 2016), (Pham et al., 2016) and (Zhu et al., 2012), magnetic leg-based robot (Mazumdar & Asada, 2009), and magnetic tank-like climbing robot (Nguyen & La, 2018). Other significant effort is from industry, such as Inuktun Inc., which developed un-touched magnetic wheel-based robots (already available on the market) for steel structure inspection like pipes, poles, containers, tanks, etc. (Inuktun, 2019). These robots may work well in flat or less curving steel surfaces, but meet difficulty when transitioning one surface to the other, or passing joints/bolts and highly curving surfaces. Different to the abovementioned climbing robots, this paper presents a new design and implementation of a roller chain-based climbing robot to provide a practical solution for steel structure inspection (bridges, poles, pipes, etc.) The proposed roller chain-like robot with 12 joints for moving and 3 pairs of joints for turning, which makes the robot becomes flexible to approach to differently complicated surfaces of steel bridges. The robot utilizing adhesion force generated by permanent magnets is able to well adhere on steel structures while moving. The roller-chain design with 15 independently controlled joints allows the robot to work well on both flat, curving surfaces and transferring points and overcome obstacles. To demonstrate the robot's working principle, it has been deployed for wide range of surfaces and experimental conditions.

2. Overall Design

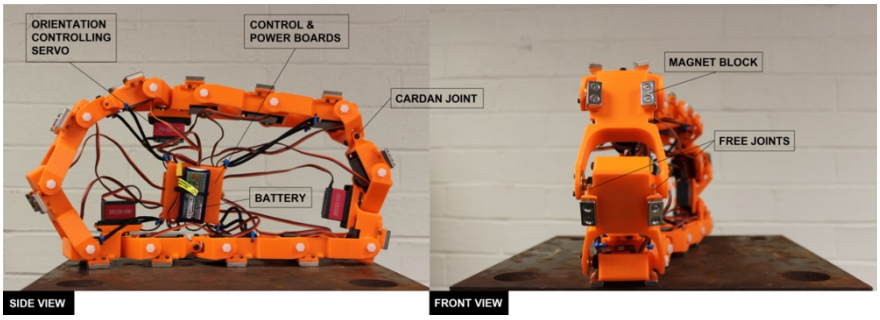

Fig 1. Overall design of robot for steel bridge inspection tasks.

The overall design of the roller chain-like robot is depicted in Fig. 1. The robot consists of 12 joints for forward and backward moving; and three pairs of joints for controlling the robot's direction. Kinematic structure of the robot is illustrated in Fig. 2. The robot moves by collaboration of 12 joint angles (1 to 12) that are driven via 12 servo motors. For turning, when robot gets state like Fig. 3, joint pairs (1.1 and 2.1) drive the robot turning left or right with 90 degrees range, in which, joints 1.1, 1.2 and 1.3 are active joints while 2.1, 2.2 and 2.3 are passive-cardan joints. Cardan joints are necessary in case the active and passive joints are not coaxial when the robot turns. With three pairs, robot can turn triple times per moving round. On each moving joint, there are two magnet blocks, which create adhesion force for the robot. The magnet blocks are integrated through the free joints to help the robot approach every surface contour effectively by manipulating natural characteristic of magnet field. The surface with largest force will expose before approaching magnetic materials as Fig. 4. The designed robot can work well on different surface contours as shown in Fig. 5.

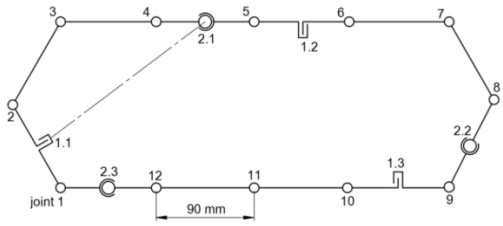

Fig 2. Robot kinematics.

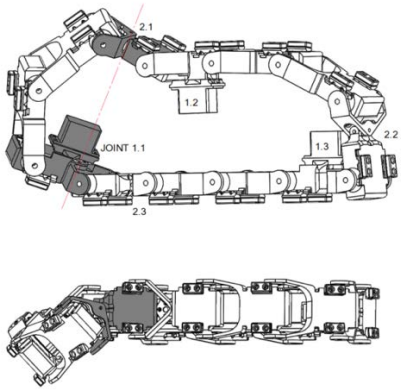

Fig 3. Robot turns left.

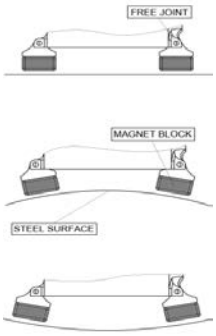

Fig 4. Magnet states before approaching steel surfaces.

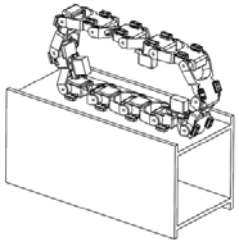

(a) Robot moves on flat surface.

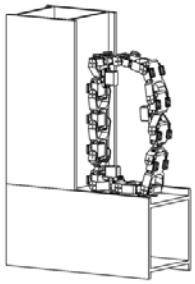

(b) Robot tranfers between two surfaces.

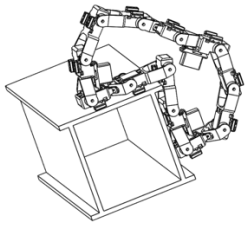

(c) Robot tranfers to other surface with obtacle.

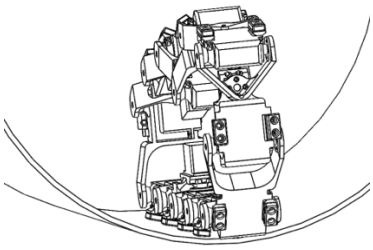

(d) Robot moves on curving surface.

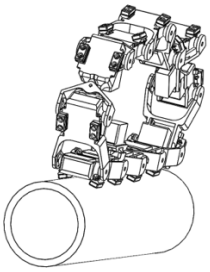

(e) Robot moves on cylinder steel surface.

(f) Robot moves on circumferential direction of cylinder object.

Fig 5. Robot's locomotion on different surface contours.

3. Magnetic Force Analysis

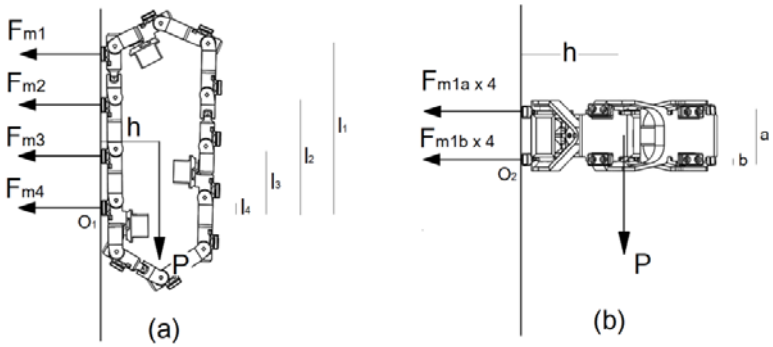

Fig 6. a) Robot attachs verically to surface; b) Robot attachs horizontally to surface.

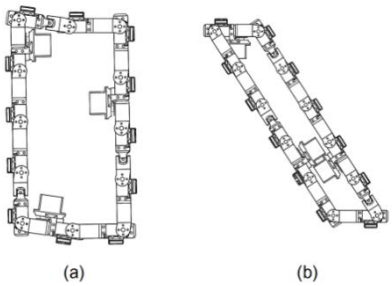

Fig 7. a) *h* max; b) *h* min.

Let *P* be the robot's total weight (*P* = *mg*, where *m* is the robot's mass, and *g* is the gravitational acceleration). Let F_m be the magnetic adhesion force, and *N* be the reaction force. Let l_1 *to* l_4 be the distance between first to last magnet block contacting to the surface to point O_1, and *h* be the distance between the center of mass to the surface (Fig. 6(a)). Moment at point O_1 is calculated as follows:

$$\sum M_{O_1} = P*h-\left(F_{m1}*l_1+F_{m2}*l_2+F_{m3}*l_3+F_{m4}*l_4\right)=0\rightarrow F_{mj}=\frac{P*h}{l_1+l_2+l_3+l_4}.$$

In case 2, Fig. 6(b), $F_{m1a}=F_{m1b}=\frac{F_{m1}}{2}$. Moment at point O_2 is calculated as follows:

$$\sum M_{O_2} = P*h-\left(4F_{m1a}*\mathrm{a}+4F_{m1b}*b\right)=0\rightarrow F_{mj}=\frac{P*h}{2\left(a+b\right)}.$$

Following the proposed design, *a* = 5.2 cm, *b* = 0.635 cm, and l_1= 28.57 cm, l_2= 19.47 cm, l_3= 9.1 cm, l_4= 1.27 cm: $\frac{P*h}{l_1+l_2+l_3+l_4}<\frac{P*h}{2\left(a+b\right)}$.

To avoid turn-over failure, the magnetic force of the magnet block: $F_{mj}>\frac{P*h}{2(\mathrm{a}+\mathrm{b})}$.

In different locomotions, the robot shape can be changed as illustrating in Fig. 7, which led to the change of *h* as well. $F_{mj} > \frac{P*h_{max}}{2(a+b)}$ (Fig. 7(a)). Therefore, to avoid both sliding and turn-over failures, the robot's magnetic force of each magnet block should satisfy:

$$F_{m_j}(j=1:n) > \max\left\{\frac{2.5P}{n}; \frac{P*h_{max}}{2(a+b)}\right\}. \quad (1)$$

Following the proposed design, P = 30 N, h_{max} = 13 cm, n = 4.

$$F_{m_j}(j=1:4) > \max\left\{\frac{2.5*30}{4}; \frac{30*13}{2*(5.2+0.635)}\right\} = 33.42(N).$$

4. Motor Torque Analysis

Position of magnet block is very important. It should be located in the position describing in Fig. 8. In both cases, when $i_1 \neq i$ (Fig. 9 and Fig. 10) the servo can not be optimal for the moment.

- $i > i_1$, we can see $x < x_1$, which means servo 4 bears more load from $F_{m1,}F_{m2,}F_{m3,}$ when moving.
- $i < i_1$, the arm is longer, which makes greater moment for the servo.

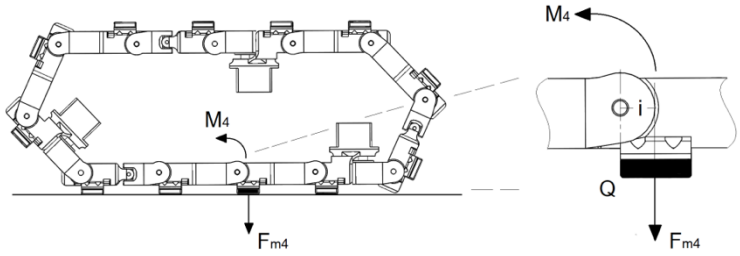

Fig 8. Magnet block position analysis.

In order to make the robot move, the force created by the servo should win the adhesion force of the last permanent magnet and the steel surface. As shown in Fig. 9, denote *M* as the torque of one motor, *Q* is rotation fulcrum, and *i* is the arm from F_{mj} to *Q*. The required moment is satisfied:

$$M_i > i*F_{mj} \quad (2)$$

i = 1.27 cm, selected magnet force F_{mj} = 80 (N) satisfied condition (1). M_i > 101,6 (N.cm).

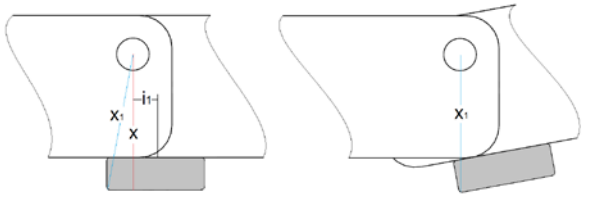

Fig 9. When $i > i_1$.

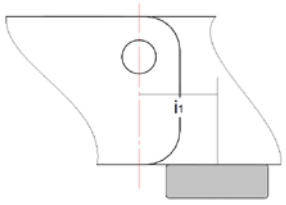

Fig 10. When $i < i_1$.

5. Experiment results

In order to measure the adhesion force created by permanent magnet, we have setup an environment as follows. The robot's body - whose mass is *m* = 3kg - is placed on top of a flat steel surface while it is connected to a scale through an inelastic wire. We create a pull force onto

the scale trying to lift the robot off the surface (similar setup to Fig. 13 in Nguyen & La, 2018). At the time the robot is about to be off the surface, the force applied to the scale is equal to the sum of robot's weight and the magnetic pull force. Denote F_{pull} as the force we applied onto the scale, M is the value shown on the scale while P is the weight of robot's body, and F_{mag} is the magnetic force. With g = 10m/s2, $P = mg$ = 30N and $F_{pull} = Mg = 10M$, we can calculate magnetic adhesion force as follows $F_{pull} = P + F_{mag} \Rightarrow F_{mag} = 10M - 3$(N). The adhesion force masurement data is shown in Fig. 11-12.

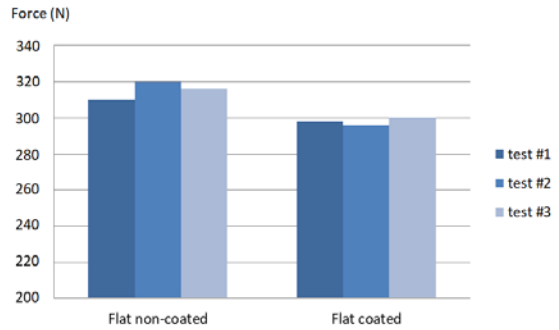

Fig 11. Adhesion force on flat surfaces.

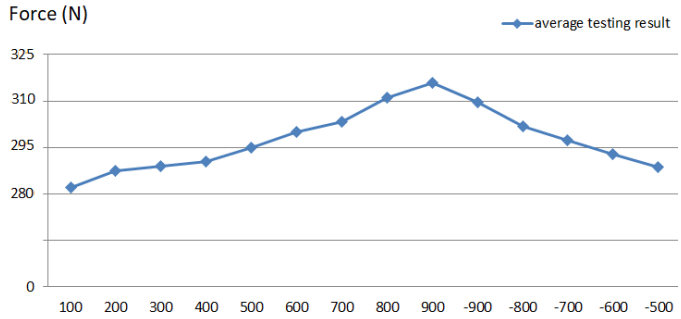

Fig 12. Adhesion force on curving surfaces with different radii.

From (1), the minimum adhesion force = n* F_{mj} (theory)= 4* 62.9=251,6 N. From (2), the maximun adhesion force of robot= n* F_{mj} (selected)= 4* 80 = 320 N as shown in Fig. 11-12.

The climbing tests were performed on both steel structures and a steel bridge (Fig. 13-15). In both cases, the robot was able to adhere strongly on the steel surface during its motion.

Fig 13. Climbing tests on steel structures. Video demonstration: https://ara.cse.unr.edu/?page_id=11

Fig 14. Climbing tests on a steel bridge at UNR's campus: https://www.youtube.com/watch?v=VoE4W5r__no&feature=youtu.be

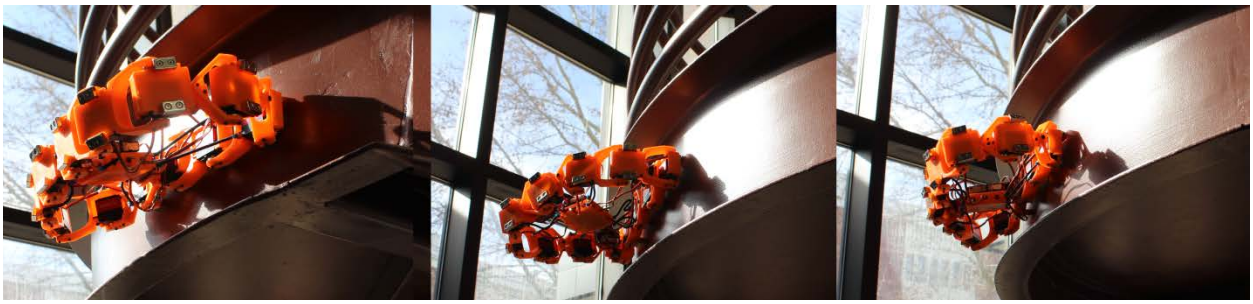

Fig 15. Climbing tests on paint-coasted steel structures.

6. Conclusions

The paper presents a new design of the climbing robot for steel bridge inspection and evaluation. The robot is designed following the roller-chain based concept in order to maximize the flexibility of the robot body. The proposed design allows the robot to climb smoothly on different steel structures and pass the joints safely. The detail of mechanical design together with the analysis of magnetic and motor forces has presented. Experimental results conducted on both steel structure and steel bridge have shown that the robot can adhere well on different steel surfaces (flat, curving, paint coasted) while moving or passing the joints. In the future work, the robot will be equipped with robotic sensors (e.g., global positioning system, inertial measurement unit, infrared, hall-effect) for autonomous localization and safe navigation on the steel structures. In addition, non-destructive evaluation sensors and visual camera will be integrated with the robot for data collection and inspection of steel structures and bridges.

References

FHWA (2016). U.S. Department of Transportation Federal Highway Administration, "National bridge inventory data," Available at: http://www.fhwa.dot.gov/bridge/nbi.cfm, accessed January 30, 2016.

Golden Gate Bridge (2018). Crews inspect condition of golden gate bridge's towers, April 30, 2018. https://www.nbcbayarea.com/on-air/as-seen-on/Crews-Inspect-Condition-of-Golden-Gate-Bridge_s-Towers_Bay-Area-481315951.html.

Pham, H. N, La, M. H., Ha, Q. P, Dang, N. S., Vo, H. A, and Dinh, H. Q. (2016). Visual and 3d mapping for steel bridge inspection using a climbing robot. *In The 33rd Intern. Symposium on Automation and Robotics in Construction and Mining (ISARC)*, pages 1–8, July 2016.

Pham, H. N., and La, M. H. (2016) Design and implementation of an autonomous robot for steel bridge inspection. *In 54th Allerton Conf. on Comm., Con., and Comp*., pages 556–562, Sept 2016.

La, M. H., Dinh, H. T., Pham, H. N., Ha, P. Q., and Pham, Q. A. (2018) Automated robotic monitoring and inspection of steel structures and bridges. *Robotica*, 37(5): 947–967, May 2019.

A. Mazumdar and H. H. Asada (2009). Mag-foot: A steel bridge inspection robot. *IEEE/RSJ International Conference on Intelligent Robots and Systems* (IROS), pages 1691–1696, Oct 2009.

Zhu, D., Guo, J., Cho, C., Wang, Y., and Lee, L. (2012). Wireless mobile sensor network for the system identification of a space frame bridge. *IEEE/ASME Trans. on Mechatronics*, 17(3):499–507, June 2012.

Nguyen, T. S., La, M. H. (2018). Development of a Steel Bridge Climbing Robot, *Robotics (cs.RO), arXiv:1803.08209 [cs.RO]*, pp. 1-8, September, 2018.

Inuktun (2019). Versatrax 150™. Available at: http://inuktun.com/en/products/. Accessed on March 20th, 2019.